GEOMORPHOMETRY 2020 PERUGIA, ITALY JUNE 22 - 26 2020
PARTNERS SPONSORS

# An optimization of triangular network and its use in DEM generalization for the land surface segmentation

Richard Feciskanin[§], Jozef Minár
Faculty of Natural Sciences
Comenius University in Bratislava
Ilkovičova 6, 842 15 Bratislava, Slovakia
[§] richard.feciskanin@uniba.sk

*Abstract*—**Appropriate generalization of digital elevation model (DEM) is important for the land surface segmentation. We tested some methods of generalization based on irregular triangular networks. Based on the theory of an optimal triangle for (land) surface representation, suitable methods simplifying triangle networks have been identified. The *quadric error metrics simplification* algorithm was used to generalize surface models. It belongs to the decimation algorithms developed in computer graphics, however the use of it for land surface modeling is rare. Suitability of the method for the land surface segmentation was evaluated for a variety of models created at different generalization levels. Numerical expression of the concentration of the third-order parameter values (curvature changes) around zero ($K_0$) was used as an indicator of the suitability. The hypothesis that the affinity of higher-order variables to a constant value should be significantly higher for real land surfaces with elementary forms than for mathematical surfaces was confirmed. The resulting $K_0$ values are significantly lower in the artificial surface than in the real surface model, however only to a threshold limit of generalization.**

## I. Introduction

The question of scale and resolution is very important in geomorphological mapping. One of the major issues of quantitative modeling and analysis of the land surface is filtering to denoise, generalize, and decompose DEMs into components of different spatial scales [1]. When a coarser analytical scale is required, the original finer-resolution DEM needs to be generalized or simplified to reduce data redundancy [2].

A resampling method is one of the most widely used methods for DEM generalization, which requires averaging the neighboring cells of a high-resolution, square-grid DEM into a series of lower-resolution data sets. This method will inevitably have a peak-clipping and valley-filling smoothing effect [3]. Other groups of grid-based DEM generalization methods include wavelet transform, morphology-based, and drainage-constrained methods, each of them with its own difficulties [4].

The polynomial least squares fitting method with a changing calculation window size was used to generalize gridded data for hierarchical land surface segmentation in [5]. In this paper, we present the use of generalized triangular irregular networks (TIN) with different level of details for the same purpose. TIN allows to simplify the detailed model so that the resulting model retains as much information about the shape of the modeled surface as possible. The spatial structure of the TIN can represents the modeled surface very efficiently and yet accurately when designed with respect to the shape of the modeled surface.

Generalization algorithms developed for land surface modeling are mostly used to create a TIN model from a regular grid. These include traditional, still popular: The Fowler and Little algorithm [6], the Very important points algorithm [7], the Drop heuristic method [8]. Similarly, other algorithms presented in [9-12, 4] use various techniques to find the most appropriate (important) points for describing the land surface.

Generalization algorithms based on TIN are more widespread outside the land surface modeling domain. They are especially widespread in the computer graphics. In contrast to the algorithms mentioned above, they primarily focus on the overall shape fidelity of the simplified model. [13] evaluated simplification methods in computer graphics as mature almost two decades ago. Unlike grid-based method, TIN-based methods from computer graphics are exceptionally used in the land surface modeling.

## II. Methods

### A. Optimal triangle

When optimizing the triangle network, we start from the theoretical assumption of an optimal triangle. [14] defines an optimal triangle whose plane has the same normal as the land surface at its centroid. A simpler but sufficiently precise description of this relationship will allow the replacement of part of the land surface with an osculating paraboloid with a vertex on land surface at the triangle centroid: Then it follows from the

*Richard Feciskanin and Jozef Minar (2020) An optimization of triangular network and its use in DEM generalization for the land surface segmentation:*
*in Massimiliano Alvioli, Ivan Marchesini, Laura Melelli & Peter Guth, eds., Proceedings of the Geomorphometry 2020 Conference, doi:10.30437/GEOMORPHOMETRY2020_2.*

above condition that the plane of the optimal triangle is parallel to the tangent plane of the surface (osculating paraboloid) at the triangle centroid (Fig. 1). The intersection of the triangle plane and the paraboloid is the same as Dupin indicatrix [15]. Consequently, the optimal triangle is one whose centroid lies in the center of the intersection conic. This can only be achieved in the case of an ellipse. The intersection is a circumscribed ellipse of a triangle centered in its centroid, known as the circumscribed Steiner ellipse. From the all circumscribed ellipses of the triangle, Steiner ellipse has the smallest area. It confirms the desirability of the approach. In places where Dupin indicatrix is not an ellipse, the condition cannot be fulfilled without deviation.

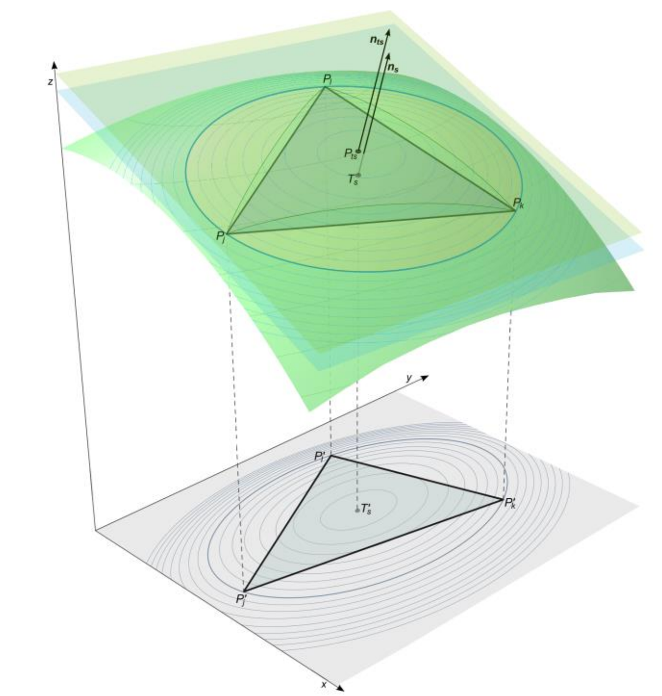

**Figure 1.** Optimal triangle representing land surface. The plane of the triangle $P_iP_jP_k$ is parallel to tangential plane of the land surface in the point $P_{ts}$ at the triangle centroid $T_s$. $n_s$, $n_{ts}$ – triangle normal and normal to surface at $P_{ts}$ are identical. Isolines of height difference between the plane of the triangle and the land surface are shown.

[16] came to the same relationship, he defined the optimum ratio of triangle ($\rho$) replacing the quadratic surface as:

$$\rho = \sqrt{\frac{\lambda_2}{\lambda_1}} \qquad (1)$$

where $\lambda_1$ and $\lambda_2$ are eigenvalues of Hessian of elevation function $z = f(x, y)$. [17] defines a triangle aspect ratio as the ratio of the principal axes of the ellipse with the smallest area that passes through the triangle vertices. Although not explicitly stated, the authors deal with the circumscribed Steiner ellipse.

### B. *Simplification algorithms*

We have identified simplification methods whose optimization conditions are in accordance with the above characteristics. These are the *quadric error metrics simplification* (*QEMS*) method presented in [18] and the *memoryless simplification* (*MS*) method introduced in [19]. Both methods were developed primarily for computer graphics, however they are also suitable for use in terrain modeling. [4] directly mention the *QEMS* method as a method for terrain simplifying, although they do not use it.

Both methods belong to the category of decimation methods. They use edge contraction to simplify the model's geometry. When contracting an edge, its two end points $V_0$ and $V_1$ are merged into a new vertex $V$. Condition for placing a new vertex is crucial. The final model consists of vertices that are not in the original data set. It allows to better maintain the local shape and has the ability to minimize the impact of random errors in the input data. The order of edges in edge list for contracting is determined by weighting of edge contraction. The contraction is repeated until the target condition is reached – most often the number of elements in the model.

The *QEMS* algorithm determines the edge contraction weight based on the value of the sum of the quadratic distance of the new vertex $V$ from the individual planes of the triangles with the original merged vertices $V_0$ and $V_1$. New vertex location is in the smallest quadratic distance from the planes of triangles with the vertices $V_0$ and $V_1$. An example of one contraction step is shown in Fig. 2. In the *MS* method, the algorithm uses the sum of tetrahedron volumes that arise from the surrounding triangles by shifting the original vertices $V_0$ and $V_1$ to a new vertex $V$ and an additional condition of preserving the volume.

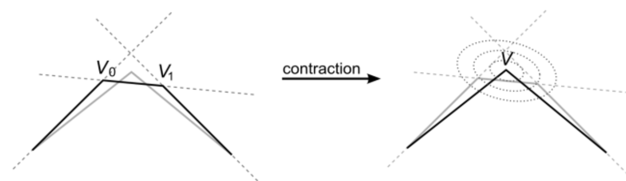


**Figure 2.** Edge contraction and new vertex localization in *quadric error metrics simplification* in 2D.

[17] showed that the aspect ratio, which is based on minimizing the quadric error, corresponds to the optimum ratio (1). Eigenvalues $\lambda_1$ and $\lambda_2$ are the extremes of principal normal curvature $\kappa_1$ and $\kappa_2$ and thus $\lambda_1 = \kappa_1$, $\lambda_2 = \kappa_2$. Extremal curvatures $\kappa_1$ and $\kappa_2$ correspond to the principal axes of Dupin indicatrix [17]. [20] presents that objective function for a new vertex localization

in *MS* bears a great deal of similarity to the quadratic form in the *QEMS* algorithm. The difference is only the weight of the triangle, they use squared value and absolute value of triangle area, respectively. This confirms that the above approach and so these methods use the same characteristics of the optimal triangle. The *QEMS* method we used to generalize the surface models.

*C. Testing triangle networks*

Third-order morphometric variables were used to describe the suitability of a triangular network for land surface segmentation. Third-order variables may be used for confirmation of land surface affinity to constant values of second-order variables, that is a precondition of existence elementary forms suitable for geomorphological mapping [21]. A quantile-based measure of kurtosis ($K_0$) presented in [21] was used as a numerical expression of concentration of data around zero

$$K_0 = \frac{\tilde{x}_{95} - \tilde{x}_5}{\tilde{x}_{0+5} - \tilde{x}_{0-5}} \qquad (2)$$

where $\tilde{x}_{95}$ and $\tilde{x}_5$ are percentiles representing the spread of the set disregarding extreme values and $\tilde{x}_{0+5}$ and $\tilde{x}_{0-5}$ represent the fifth percentiles on the right and on the left from the zero value. The values of slope line (s) and contour line (c) changes of profile curvature $(k_n)_s$ and tangential curvature $(k_n)_c$ denoted $(k_n)_{ss}$, $(k_n)_{sc}$, $(k_n)_{cc}$, $(k_n)_{cs}$ were used.

We have determined the partial derivatives up to the third order for each vertex (except borders) and triangle centroids of the optimized triangular network based on the fourth order polynomial least square fitting. The input to the least square fitting were 3-ring neighborhood vertices. We calculated the summary characteristic $K_0$ from the determined $(k_n)_{ss}$, $(k_n)_{sc}$, $(k_n)_{cc}$, $(k_n)_{cs}$ values. This calculation was performed repeatedly for generalized models at different degrees of generalization.

[21] presents the hypothesis: The affinity of higher-order variables to a constant value should be significantly higher for real land surfaces with elementary forms or other structures than for mathematical surfaces. To confirm this, the same calculation of $K_0$ was made on generalized models of the artificial surface.

## III. RESULTS AND DISCUSSION

The basic DEM of the surveyed area was created from a photogrammetric mapping in the form of a grid of 166×163 (27058) cells with a resolution of 2 meters. It represents an area located on the west of Bratislava, Slovakia, around the hill of Slovinec. The artificial surface model was calculated for 241×241 (58081) points based on a mathematical formula (trigonometric polynomial) with a fictitious 5 meters resolution.

The nodes of the regular grids form the vertices of the initial triangular networks. Initial TIN was generalized to more than 100 levels up to last 30 (40 in artificial surface) triangular faces. The selected generalization levels of the models are shown in fig. 3 and 4. The ability of the algorithm to capture the most important surface shapes with a very small number of elements is evident.

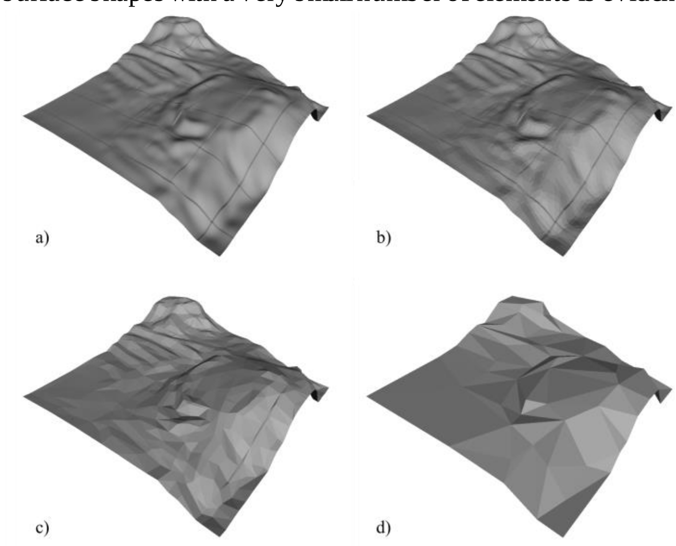


**Figure 3.** Examples of generalized models of Slovinec: a) initial model (53460 triangles), b) 5000 triangles, c) 1000 triangles d) 100 triangles.

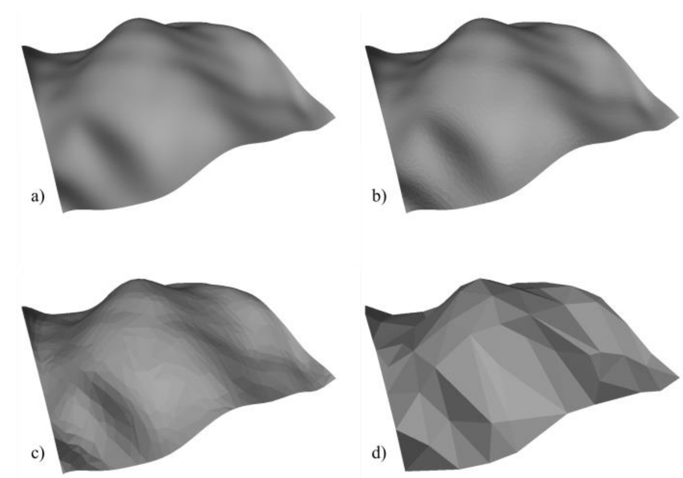


**Figure 4.** Examples of generalized artificial surface models: a) initial model (115200 triangles), b) 5000 triangles, c) 1000 triangles d) 100 triangles.

The calculated values of $K_0$ from the set of changes of curvature $(k_n)_{ss}$, $(k_n)_{sc}$, $(k_n)_{cc}$, $(k_n)_{cs}$ in each model are shown in fig. 5.

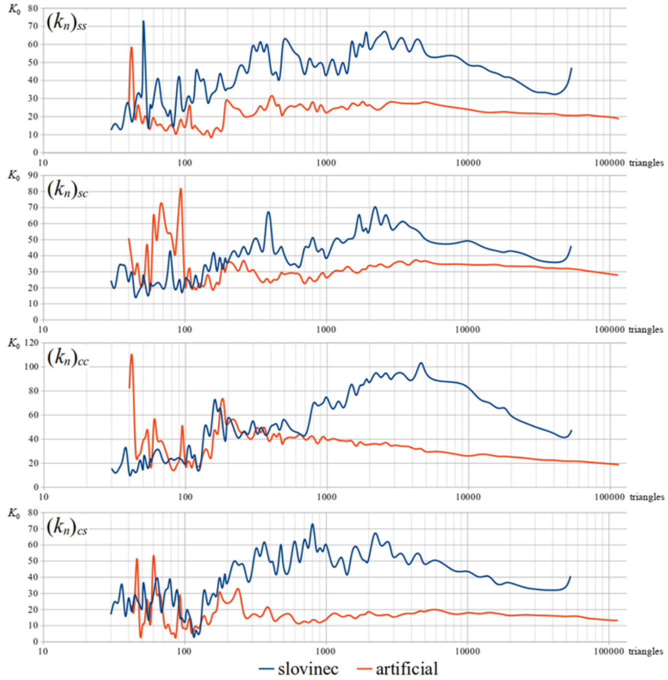


**Figure 5.** Values of $K_0$ for each types of curvature changes in the whole range of generalization.

The artificial surface has much lower values of $K_0$ up to generalization 100 – 200 triangles excluding $(k_n)_{cc}$ (~700 triangles). It points to existence of elementary forms with affinity to constant value of $(k_n)_s$ and $(k_n)_c$ and/or their parent variables – slope, aspect and altitude. Generalizations with < 200 triangles make artificial and natural surface equal in light of $K_0$. Instability of moment based $K_0$ (strong dependence on random values) for small datasets can be one reason. An artificial facets (surface of particular big triangles) is another possible reason of convergence and extremums of both (artificial and natural) $K_0$ curves.

## IV. Conclusions

The optimization of triangular network by *QEMS* method (used nearly exclusively in computer graphics till now) can be effectively used for generalization of DEM. $K_0$ index can be suitable for determination of generalization levels optimal for land surface segmentation only to a certain level of generalization, given by approach of $K_0$ curves of artificial and natural surface.

## Acknowledgment

This work was supported by the Slovak Research and Development Agency under contract APVV-15-0054.

## References


[1] Florinsky, I. V. & Pankratov, A. N., 2016. "A universal spectral analytical method for digital terrain modeling". Int. J. Geogr. Inf. Sci. 30, pp. 2506–2528.

[2] Zhou, Q. & Chen, Y., 2011. "Generalization of DEM for terrain analysis using a compound method". ISPRS J. Photogramm. Remote Sens. 66, pp. 38–45.

[3] Chen, Y., Wilson, J. P., Zhu, Q. & Zhou, Q., 2012. "Comparison of drainage-constrained methods for DEM generalization". Comput. Geosci. 48, pp. 41–49.

[4] Wu, Q., Chen, Y., Wilson, J. P., Liu, X. & Li, H., 2019. "An effective parallelization algorithm for DEM generalization based on CUDA". Environ. Model. Softw. 114, 64–74.

[5] Minár, J., Minár, J. Jr. & Evans, I.S., 2015. "Towards exactness in geomorphometry". In Geomorphometry 2015 Conference Proceedings, Edited by: Jasiewicz, J., Zwoliński, Z., Mitasova, H. and T. Hengl, Adam Mickiewicz University in Poznań, Poland.

[6] Fowler, R. J. & Little, J. J., 1979. "Automatic extraction of Irregular Network digital terrain models". ACM Comput Graphics 13, pp. 199–207.

[7] Chen, Z.-T. & Guevara, J. A., 1987. "Systematic selection of very important points (VIP) from digital terrain model for constructing triangular irregular network". Auto Carto 8. pp. 50–56.

[8] Lee, J., 1989. "A drop heuristic conversion method for extracting irregular networks for digital elevation models". Proceedings of GIS & LIS'89. pp. 30–39.

[9] Fei, L. & He, J., 2009. "A three-dimensional Douglas-Peucker algorithm and its application to automated generalization of DEMs". Int. J. Geogr. Inf. Sci. 23, pp. 703–718.

[10] Chen, Y. & Zhou, Q., 2013. "A scale-adaptive DEM for multi-scale terrain analysis". Int. J. Geogr. Inf. Sci. 27, pp. 1329–1348.

[11] Chen, Y. et al., 2016. "A new DEM generalization method based on watershed and tree structure". PLoS One 11, p. 23.

[12] Sun, W., Wang, H. & Zhao, X., 2018. "A simplification method for grid-based DEM using topological hierarchies". Surv. Rev. 50, pp. 454–467.

[13] Luebke, D. P., 2001. "A developer's survey of polygonal simplification algorithms". IEEE Comput. Graph. Appl. 21, pp. 24–35.

[14] Krcho J., 1999. "Modelling of georelief using DTM - the influence of point configuration of input points field on positional and numeric accuracy". Geogr. časopis. 1999;51(3). pp. 225-260.

[15] Günther, F., Jiang, C. & Pottmann, H., 2020. "Smooth polyhedral surfaces". Adv. Math. 363, p. 31.

[16] Nadler, E., 1986. "Piecewise linear best $l_2$ approximation on triangles". In: Chui, C.K., Schumaker, L.L. and Ward, J.D. (Eds.), Approximation Theory V, Academic Press, 499–502.

[17] Heckbert, P. S. & Garland, M., 1999. "Optimal triangulation and quadric-based surface simplification". Comput. Geom. Theory Appl. 14, pp. 49–65.

[18] Garland, M. & Heckbert, P. S., 1997. "Surface simplification using quadric error metrics". Proceedings of the 24th Annual Conference on Computer Graphics and Interactive Techniques, SIGGRAPH 1997. pp. 209–216.

[19] Lindstrom, P. & Turk, G., 1998. "Fast and memory efficient polygonal simplification". Proceedings Visualization'98.

[20] Lindstrom, P. & Turk, G., 1999. "Evaluation of memoryless simplification". IEEE Trans. Vis. Comput. Graph. 5 (2), pp. 98–155.

[21] Minár, J. et al. "Third-order geomorphometric variables (derivatives): Definition, computation and utilization of changes of curvatures". Int. J. Geogr. Inf. Sci. 27, pp. 1381–1402.